Both Spike and Background Genes Contribute to Murine Coronavirus Neurovirulence

Kathryn T. Iacono,† Lubna Kazi,‡ and Susan R. Weiss*

Department of Microbiology, University of Pennsylvania, School of Medicine, Philadelphia, Pennsylvania

Various strains of mouse hepatitis virus (MHV) exhibit different pathogenic phenotypes. Infection with the A59 strain of MHV induces both encephalitis and hepatitis, while the highly neurovirulent JHM strain induces a fatal encephalitis with little, if any, hepatitis. The pathogenic phenotype for each strain is determined by the genetic composition of the viral genome, as well as the host immune response. Using isogenic recombinant viruses with A59 background genes differing only in the spike gene, we have previously shown that high neurovirulence is associated with the JHM spike protein, the protein responsible for attachment to the host cell receptor (J. J. Phillips, M. M. Chua, G. F. Rall, and S. R. Weiss, Virology 301:109–120, 2002). Using another set of isogenic recombinant viruses with JHM background genes expressing either the JHM or A59 spike, we have further investigated the roles of viral genes in pathogenesis. Here, we demonstrate that the high neurovirulence of JHM is associated with accelerated spread through the brain and a heightened innate immune response that is characterized by high numbers of infiltrating neutrophils and macrophages, suggesting an immunopathogenic component to neurovirulence. While expression of the JHM spike is sufficient to confer a neurovirulent phenotype, as well as increased macrophage infiltration, background genes contribute to virulence as well, at least in part, by dictating the extent of the T-cell immune response.

Mouse hepatitis virus (MHV) is a member of the family *Coronaviridae*, consisting of large, single-stranded RNA viruses. Coronaviruses (CoV) cause respiratory and enteric infections in domestic animals and humans that can range from mild to severe and potentially lethal. For example, the human CoV 229E and OC43 induce mild respiratory disease, while the emergence of a novel human coronavirus, SARS-CoV, as the etiologic agent of severe acute respiratory syndrome demonstrates that a coronavirus can also cause serious, potentially lethal infections in humans (9, 13). MHV also induces disease with a wide range of clinical pathologies that include neurological, hepatic, enteric, and respiratory dysfunctions, with outcomes dependent upon the viral strain administered, the route of infection, and the strain and age of the animal (5). Delivery of virus to susceptible animals via the intracranial (i.c.) or intranasal route serves as a model for studying both acute and chronic virus-induced neurological disease. Two naturally occurring strains, JHM and A59, have been shown to induce very different pathologies following i.c. infection. The JHM strain of MHV, which has been previously referred to as MHV-4 (2) or MHV$_{SD}$ (23), was isolated from an animal having hind-limb paralysis and is highly neurovirulent in weanling C57BL/6 (B6) mice. Fatal encephalitis is induced in most mice following inoculation with viral doses as low as 2 PFU (6, 17). Similar administration of the less neurovirulent, laboratory-adapted A59 strain induces mild encephalitis concomitant with moderate hepatitis. While resolution of encephalitic symptoms occurs with clearance of the A59 strain, persisting viral RNA can still be detected, and infected animals undergo chronic primary demyelination.

Viral pathogenesis is a complex phenomenon that is determined by both viral genetics and the host immune response. The comparison of the highly neurovirulent JHM and mildly neurovirulent A59 strains of MHV has allowed us to study the balance and interrelationship of these factors within the central nervous system (CNS). We have selected JHM/A59 chimeric recombinant viruses; these viruses have been used to delineate the roles that both spike and background genes play in the clinical outcome. Previous studies from our laboratory using isogenic recombinant viruses differing only in the viral spike gene have demonstrated that the spike gene, encoding the protein responsible for attachment to the host cell and subsequent fusion and entry, is a major determinant of MHV neurovirulence. A highly neurovirulent phenotype was conferred upon the recombinant A59 virus, in which the spike gene was replaced by that of JHM. This chimeric virus (SJHM/RA59) was characterized by a 3-log$_{10}$-unit decrease in the intracranial 50% lethal dose (LD$_{50}$), increased rate of viral-antigen spread and inflammation, and a more robust T-cell immune response than wild-type recombinant A59 (RA59) (26, 28, 31). The chimeric virus was, however, not as virulent as wild-type recombinant RJHM. Analysis of JHM/A59 chimeric viruses demonstrated that one or more genes within the 3′ end of the JHM genome are necessary for the extremely high neurovirulence of JHM (15; S. Navas-Martin and S. R. Weiss, unpublished data). In order to further understand the contributions of both viral spike and background genes to the process of neurovirulence, we have compared, in addition to RA59 and SJHM/RA59, another set of isogenic recombinant viruses differing only in spike: wild-type JHM (RJHM) and the

* Corresponding author. Mailing address: Department of Microbiology, University of Pennsylvania, School of Medicine, 36th Street and Hamilton Walk, Philadelphia, PA 19104-6076. Phone: (215) 898-8013. Fax: (215) 573-4858. E-mail: weisssr@mail.med.upenn.edu.
† Present address: Department of Pathology and Laboratory Medicine, University of Pennsylvania, School of Medicine, Philadelphia, PA.
‡ Present address: Department of Medicine, University of Pennsylvania, School of Medicine, Philadelphia, PA.
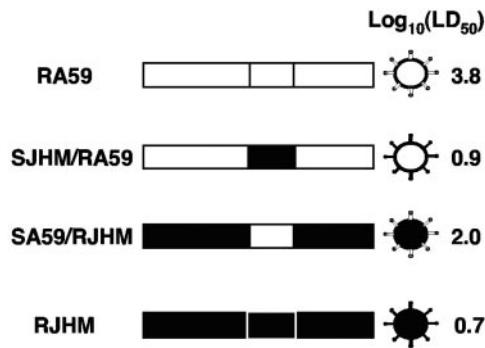
FIG. 1. The genomes of recombinant MHVs. The genomes of parental recombinant strains, RJHM and RA59, as well as those of chimeric viruses with exchanges of spike genes, SJHM/RA59 and SA59/RJHM, are all shown. LD_{50} values, following intracranial inoculation, are provided to demonstrate the contribution of the viral spike protein to the level of neurovirulence.

chimeric virus SA59/RJHM (with the A59 spike protein expressed within the JHM background). Evaluation of the CNS immune infiltrates was performed through a series of fluorescence-activated cell sorting (FACS) analyses with antibodies specific for both innate and adaptive immune mediators. We demonstrate here that the type and extent of the immune response segregate with viral genes, with background genes directing the induction of T cells and the viral spike directing the infiltration of macrophages. The combination of rapid and extensive spread through the CNS with the lack of induction of a significant T-cell response results in the extremely high lethality of JHM, typified by heightened recruitment of neutrophils.

MATERIALS AND METHODS

Recombinant viruses. All the viruses used were recombinant viruses selected by targeted recombination (21, 26); schematic diagrams are shown in Fig. 1. They included wild-type A59 (RA59; also referred to in the literature as wtR) (26, 27) and RJHM (21), as well as chimeric A59 with the JHM spike gene substituted for that of A59 (SJHM/RA59, previously referred to as S4R) (26, 27) and chimeric JHM with the A59 spike gene substituted for that of JHM (SA59/RJHM) (1).

Inoculation of mice. All animal experiments were performed with 4-week-old, MHV-free, male B6 mice (National Cancer Institute, Bethesda, MD). The mice were anesthetized with isoflurane (Abbott). For i.c. inoculation, 20-µl volumes of virus were injected into the left cerebral hemisphere after dilutions were made in phosphate-buffered saline (PBS) supplemented with 0.75% bovine serum albumin (BSA). Control mice were mock infected with uninfected cell lysates at a similar dilution.

Virulence assays. The 50% lethal dose was calculated as previously described (11). Four-week-old B6 mice were inoculated intracranially with four serial dilutions of each recombinant virus. Ten animals per viral dilution were used. The mice were observed for a period of 21 days for morbidity and mortality. LD_{50} values were calculated from two independent experiments by the Reed-Muench method (30).

Virus replication in mice. For determination of viral replication levels in the brain and liver, five mice were inoculated intracranially with each virus per time point. The mice were sacrificed at days 3, 5, and 7 postinfection (p.i.) and perfused via cardiac puncture of the left ventricle with 10 ml sterile PBS, and their brains and livers were removed. The left half of the brain and a lobe of the liver were each placed into separate tubes containing 2 ml of isotonic saline supplemented with 0.167% gelatin (gel saline). The organs were weighed and stored at −80°C until they could be homogenized and titered by determining plaque assays on L2 cells as previously described (14).

Immunohistochemistry. For analysis of viral-antigen spread, mice were sacrificed at various time points as described above, and one-half of the brain, as well as part of the liver, was fixed in 10% phosphate-buffered formalin. The formalin-fixed tissues were embedded in paraffin, sectioned, and left unstained for immunohistochemistry. Sections from mock-infected animals were used as controls. The tissues were first deparaffinized and then rehydrated. Immunohistochemistry was carried out by the avidin-biotin-immunoperoxidase technique (Vector Laboratories, CA), using diaminobenzidine tetrachloride as a substrate and hematoxylin as a counterstain. The sections were incubated with a monoclonal antibody directed against the nucleocapsid (N) protein of the MHV-JHM strain (a gift of J. Leibowitz, Texas A&M University) at a 1:20 dilution. Three sagittal sections per virus obtained from each of three individual animals were studied in a blinded manner. For each section, similar regions of the brain were examined and compared.

Isolation of mononuclear cells from the brain. Mononuclear cells from the brain were prepared as previously described (4, 25). Briefly, mice were sacrificed on days 5 and 7 post-intracranial inoculation. Cells harvested from five brains per infected group were pooled and passed through a 30% Percoll gradient, followed by passage through a cell strainer (70-µm pore diameter) (Becton Dickinson). The cell suspension was layered on top of a 3-ml cushion of Lymphocyte-M (Cedarlane Laboratories), and viable cells were removed from the interface, washed three times with 1× PBS, and counted.

Determination of cell surface marker expression by FACS analysis. Individual cell populations were identified using FACS by analyzing the expression of cell surface antigens with the aid of fluorescently conjugated monoclonal antibodies. For surface antigen staining, 1×10^5 cells/well were plated in 96-well round-bottom plates and washed three times in 1% BSA-PBS. Nonspecific binding of antibodies was blocked with a 15-min incubation at 4°C with a 1:200 dilution of anti-CD16/CD32 (Fcγ III/II receptor, clone 2.4G2). Leukocytes were identified using fluorescein isothiocyanate (FITC)-conjugated anti-CD45 (leukocyte common antigen, clone 30-F11). Double staining with anti-CD45 in combination with either anti-CD4 (clone RM4-5), anti-CD8a (clone 53-6.7), anti-NK1.1 (NKR-P1B and NKR-P1C), anti-Ly-6G (Gr-1) (BD-Pharmingen), or anti-F4/80 (Caltag Laboratories) antibody further differentiated the leukocyte population into $CD4^+/CD8^+$ T-cell, natural killer (NK) cell, neutrophil, and macrophage populations, respectively. Cells were incubated with the aforementioned antibodies at 4°C for 1 h, washed three times in 1% BSA-PBS, and fixed in 2% paraformaldehyde solution. FACS analyses were performed using the FACScan flow cytometer (Becton Dickinson), gating on all living cells. The total number of each cell type per mouse brain was derived by multiplying the percentage of positive gated cells for a given surface antigen by the total number of viable cells isolated per brain.

Intracellular IFN-γ staining. Intracellular gamma interferon (IFN-γ) secretion was assayed in response to stimulation with specific peptides, as previously described. Brain-derived mononuclear cells (1×10^6) were cultured with 10 units human recombinant interleukin-2 and 1 µl/ml brefeldin A (Golgiplug; PharMingen), either with or without 1 µg/ml viral-epitope-specific peptide, in a total volume of 200 µl of RPMI 1640 medium supplemented with 5% fetal calf serum for 5 h at 37°C. The cells were then stained for surface expression of CD8 using monoclonal antibodies specific for CD8a (clone 53-6.70) (PharMingen). After surface staining, intracellular IFN-γ was detected by first fixing and then permeabilizing cells using the Cytofix/Cytoperm kit (PharMingen), followed by staining them with a FITC-conjugated monoclonal rat anti-mouse IFN-γ antibody (clone XMG 1.2; PharMingen). The cells were analyzed using a FACScan flow cytometer (Becton Dickinson). The percentage of virus-specific IFN-γ-positive $CD8^+$ cells was determined following FACS analysis and is expressed as the number of double-positive cells divided by the total number of $CD8^+$ cells.

In vivo neutrophil depletion. Four-week-old B6 mice were injected intraperitoneally to either deplete circulating neutrophils (treatment with RB6-8C5) or inhibit their respiratory-burst function (treatment with the inducible nitric oxide synthase inhibitor aminoguanidine hemisulfate [Sigma]). PBS injections served as a control. For the depletion of circulating neutrophils and PBS controls, 200 mg of RB6-8C5 ascites fluid or 150 µl PBS was administered every other day beginning at day −1 and continuing through the experimental course. For the inhibition of inducible nitric oxide synthase, aminoguanidine hemisulfate was administered at a dose of 250 mg/kg body weight intraperitoneally twice a day, beginning at day −1, with 1% aminoguanidine (wt/vol) administered continuously via the water supply by the method of Andrews et al. (1). All animals were infected i.c. with 10 PFU of RJHM at day zero and monitored for morbidity and mortality over the experimental course. The animals were sacrificed at day 5 p.i., and both brains and spleens were harvested. Pooled mononuclear cells from each organ were isolated and analyzed by FACS analysis to determine neutrophil levels.

Detection of neutrophils within the brain parenchyma. Immunofluorescent staining was performed to determine the relative number of neutrophils within the brain parenchyma. Frozen sagittal sections from mice were prepared on days

3, 5, and 7 postinfection. Sections were fixed in ice-cold 95% ethanol for 15 min at −20°C, followed by a 5-min wash in ice-cold PBS. Nonspecific associations were prevented by blocking the sections for 15 min in 1.5% goat serum prepared in PBS (serum block) at room temperature, followed by two separate 15-min incubations with avidin and biotin (Vector Laboratories). Purified rat anti-Ly6G (BD Pharmingen; clone 1A8) and rabbit anti-MHV A59 polyclonal antibodies were diluted 1:100 in serum block and incubated for 2 h in a humidified chamber at room temperature. Slides were washed three times with PBS prior to incubation with species-specific anti-rat (neutrophils) and Texas Red-conjugated anti-rabbit (viral antigen) secondary antibodies in a humidified chamber for 1 h at room temperature. Fluorescent detection of neutrophils was achieved following a 30-min incubation with FITC-conjugated avidin. The sections were washed twice in PBS prior to being mounted and were allowed to dry overnight at room temperature prior to visualization.

Apoptosis within the CNS: TUNEL staining. Frozen sagittal sections from animals sacrificed at day 5 postinfection after treatment with RB6-8C5 and aminoguanidine hemisulfate and from PBS-treated animals were prepared and evaluated for apoptosis by terminal deoxynucleotidyltransferase-mediated dUTP-biotin nick end labeling (TUNEL) staining (Roche), following the manufacturer's protocol with one variation. Briefly, tissue sections were fixed in 4% paraformaldehyde-PBS solution, pH 7.4, for 20 min at room temperature, followed by a 30-min PBS wash, also at room temperature. Permeabilization was performed following the method of Deng et al. (8) rather than the kit instructions. Immersion of slides in 80°C preheated 0.5% Triton X-100–0.01 M PBS (pH 7.4) solution for 20 min was shown to improve the TUNEL method without inducing false positives. The TUNEL reaction mixture was prepared by mixing 50 μl of enzyme solution with 450 μl of labeling solution; 50 μl of the resultant mixture was added to each section. The sections were incubated in a humidified chamber at 37°C for 60 min in the dark. Slides were washed three times with PBS prior to being coverslipped. Brain sections from mock-infected mice served as both positive and negative controls. The absence of any FITC signal in the negative control demonstrated the efficacy of the protocol used. For the positive control, brain sections were incubated with 3 U/ml DNase I prepared in 50 mM Tris-HCl, pH 7.5, supplemented with 1 mg/ml BSA and incubated for 10 min at room temperature to induce double-strand DNA breaks prior to the labeling procedure.

RESULTS

Virulence of recombinant viruses. We have previously described the selection of recombinant viruses, RA59, SJHM/RA59, SA59/RJHM, and RJHM, using targeted recombination technology (21, 26, 40) (Fig. 1 shows a schematic representation of these viruses). The study of the virulence properties of SJHM/RA59 has shown that the introduction of the JHM spike gene is sufficient to confer higher virulence on A59 (26); however, the replacement of the JHM spike with the A59 spike did not completely alter JHM virulence as determined by calculation of LD_{50} values following intracranial inoculation (21).

To obtain a more detailed evaluation of the virulence properties of the recombinant viruses, B6 mice were inoculated intracranially with 10 PFU of SA59/RJHM, SJHM/RA59, RJHM, and RA59 and observed daily for signs of disease and mortality. The data, plotted as percent survival as a function of time, are shown in Fig. 2. When challenged with a low viral dose, as expected, mice infected with RA59 did not succumb to disease and showed 100% survival, while mice infected with the same dose of SA59/RJHM showed minimal symptoms and had a survival pattern similar to that with RA59. Both JHM spike-expressing viruses demonstrated high degrees of lethality, with 70% of RJHM-infected animals dying by day 9 p.i. and 60% of SJHM/RA59-infected mice dying by day 11 p.i. Thus, virulence largely segregates with the spike gene; in fact, since JHM and SJHM/RA59 are both highly lethal, their LD_{50} values following intracranial inoculation are not distinguishable.
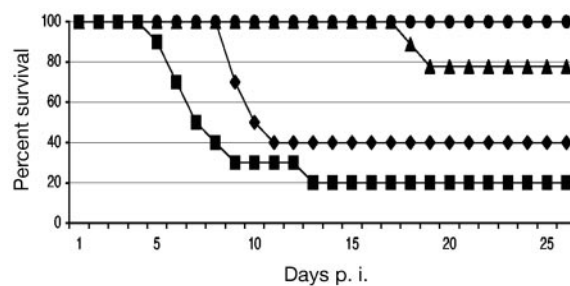

FIG. 2. Survival rates following intracranial infection. C57BL/6 mice (10 per virus) were inoculated intracranially with 10 PFU of RJHM (squares), SJHM/RA59 (diamonds), RA59 (circles), or SA59/RJHM (triangles); monitored daily for mortality; and plotted as percentages of mice surviving as a function of days postinfection. The values presented are representative of three independent experiments.

However, when the time to death is noted, it is clear that the presence of JHM background genes does confer increased virulence over viruses with A59 background genes; this is the case for viruses expressing either spike gene.

Replication of recombinant viruses in brains and livers. Intracranial infections of 4-week-old mice with SA59/RJHM, SJHM/RA59, RJHM, and RA59 were compared to determine whether the extents of replication in the brain and liver correlated with virulence. Mice were sacrificed at days 3, 5, and 7 postinfection; brains and livers were isolated and homogenized; and titers were determined from homogenates as described in Materials and Methods. Infectious viral titers in the brain and liver, respectively, were measured at each time point using a standard plaque assay (data not shown). Following intracranial inoculation virus-titering experiments demonstrated that all four recombinant viruses replicated to similar extents in the brain, yet histological analyses showed that disparities existed between the levels of viral antigen within the brain parenchyma (Fig. 3). This is in agreement with previous observations from our laboratory (26) that for MHV infections, the level of infectious virus in the brain is not a reliable indicator of the degree of virulence. We speculate that the cerebrospinal fluid serves as a conduit for independent cell-cell spread that allows the spotted histological patterns we observed, as well as the inflated viral titers obtained following analyses of brain homogenates. In contrast to the observation in the brain, the level of MHV replication in the liver is a good indication of the ability to cause disease in that organ (20). Hepatotropism was expected to segregate with the A59 spike gene, as both JHM and SJHM/RA59 have been shown to be poorly hepatotropic. However, only RA59, and not the SA59/RJHM chimera, was capable of replicating in the liver at this low dose, thus indicating that both spike and nonspike genes contribute to viral tropism in what appears to be a tissue-specific manner (21) and further supporting the notion that JHM background genes may suppress the ability of viruses expressing the A59 spike to infect the liver.

Spread of viral antigen in the brain. To determine the location and extent of viral spread in the brain, samples harvested from mice infected with the recombinant viruses SA59/RJHM, SJHM/RA59, RJHM, and RA59 were processed for immunohistochemistry. Sagittal brain sections (three per ani-
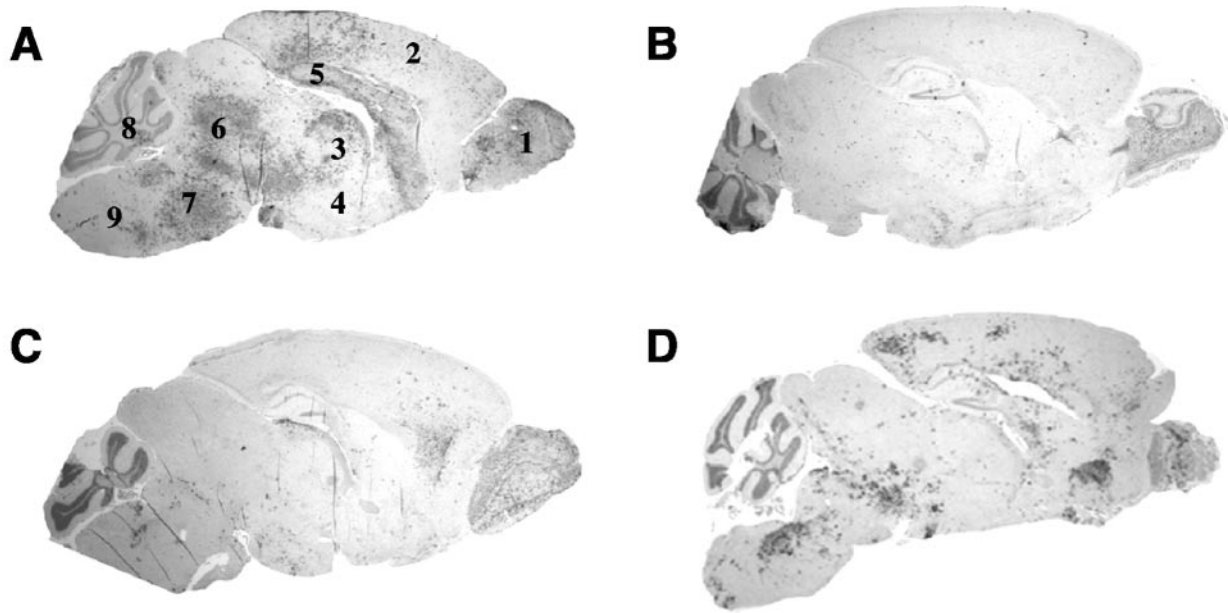
FIG. 3. Viral spread within the brain. C57BL/6 mice were infected with 10 PFU of virus, RJHM (A), SA59/RJHM (B), RA59 (C), or SJHM/RA59 (D), intracranially and sacrificed 5 days postinfection. Sagittal brain sections were prepared and stained by immunohistochemistry using a monoclonal antibody directed against viral nucleocapsid. Representative images are shown at ×1 magnification. Region identities: 1, olfactory bulb; 2, cerebral cortex; 3, thalamus; 4, hypothalamus; 5, hippocampus; 6, midbrain; 7, pons; 8, cerebellum; 9, medulla.

mal per time point) were stained with monoclonal antibody raised against the viral nucleocapsid protein and examined in a blinded fashion. There were major differences among the recombinant viruses with respect to the degree of viral spread observed by day 5 p.i., the peak of viral-antigen expression. At day 5 postinfection, sections from RJHM-infected animals displayed extensive spread of viral antigen throughout the brain; though it was observed in the neocortex, olfactory bulb, and basal forebrain, the most viral-antigen-dense regions were found in the mid- and hindbrain regions. While the brain sections from SJHM/RA59-infected mice had a pattern of viral-antigen spread similar to that observed in sections from RJHM-infected mice with respect to the affected regions, the number of antigen-positive cells within these regions was dramatically lower (Fig. 3A and D) and demonstrated considerably lower levels of inflammation (data not shown). At the same time postinfection, sections from both viruses with A59 spike genes (RA59 and SA59/RJHM) exhibited much lower levels of viral antigen (Fig. 3B and C). These observations are consistent with the kinetics of mortality (Fig. 2). By day 7 postinfection, many of the RJHM-infected mice had died; this suggests that the in vivo virulence of RJHM coincides with its ability to spread more quickly through the CNS than the other viruses. These results demonstrate that although the expression of the JHM spike is sufficient to confer greater neurovirulence, as witnessed with the SJHM/RA59 infections, comparison of parental recombinants with the spike chimeric viruses clearly indicates that nonspike genes also contribute to viral-antigen spread and virulence in the CNS.

Innate immune response is influenced by both spike and background genes. The innate immune response induced with respect to the number of NK cells, macrophages, and neutro-

phils present in the brains at designated times postinfection with each of the four recombinant viruses was evaluated. To this end, infected mice were sacrificed at various times postinfection; mononuclear cells were recovered from individual brains and pooled, stained with cell-type-specific antibodies specific for each of the aforementioned populations, and quantified by flow cytometry as described in Materials and Methods. The levels of individual cell types at day 5 p.i. (the peak of viral-antigen expression) and day 7 p.i. (the peak of encephalitis) were expressed as percentages of gated cells (Fig. 4A) and as the number of cells per brain (Fig. 4B). While animals infected with RA59, RJHM, and SJHM/RA59 exhibited similar levels of NK infiltration, they differed with respect to macrophage and neutrophil populations. Both JHM spike-expressing viruses induced appreciably heightened levels of macrophage infiltration, having fourfold greater total numbers of infiltrating cells than did either A59 spike-containing virus by day 7 p.i. (Fig. 4B) What makes the two groups of viruses even more distinct is the fact that the JHM- and SJHM/RA59-infected animals did not demonstrate a mitigation of macrophage recruitment but rather showed an enhancement over the time course observed (Fig. 5B). These findings suggest that the viral spike may direct macrophage infiltration of the CNS, as well as establish a proinflammatory environment that favors retention of innate immunity over transition to adaptive immunity.

Concomitant with the elevated macrophage population within the RJHM-infected CNS was a dramatic elevation in the levels of neutrophils. Figure 5 shows the FACS plots for analysis of neutrophils from the brains of RJHM-infected mice at days 5 and 7 p.i. While neutrophils accounted for approximately 15 to 20% of the inflammatory cells in the brains of
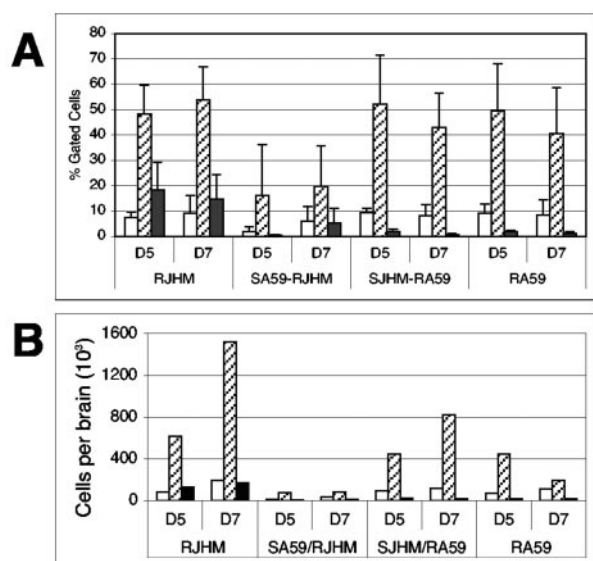
FIG. 4. Quantification of NK cells, macrophages, and neutrophils in the CNSs of infected mice. At day 5 p.i., mononuclear cells were isolated from the brains of B6 mice infected with RJHM, SA59/RJHM, SJHM/RA59, and RA59. Cells from five mice per virus were pooled and analyzed for surface antigen expression by staining them with cell-type-specific antibodies—NK1.1 for NK cells (open bars), F4/80 for macrophages (shaded bars), and Ly-6G for neutrophils (closed bars)—followed by FACS analysis. The level of each cell type is presented both as (A) a percentage of total gated cells following the collection of 10,000 FACS events and (B) the total number of each cell type per brain. The values represent the means (A and B) and standard deviations (A) of at least five individual experiments per virus.

RJHM-infected mice at both days 5 and 7 p.i., there were minimal levels of this cell type in the brains of animals infected with the other three viruses (Fig. 5 and 6). As with the macrophage population, the level of neutrophils remained high at day 7 p.i. in the brains of JHM-infected mice. The contribution of neutrophils to the process of neuropathogenesis was further

investigated via their selective depletion or by inhibiting nitrous oxide synthase (NOS) (Fig. 6). Mice were treated with the neutrophil-depleting antibody RB6-8C5 (37), the NOS inhibitor aminoguanidine, or PBS prior to and throughout the course of infection until day 5 p.i. (as described in Materials and Methods), at which time the mice were sacrificed. Immunofluorescent staining of adjacent frozen sagittal sections from PBS-treated animals demonstrated the overlap of neutrophil populations with areas of viral-antigen expression (Fig. 6A, B, and C) and apoptosis (Fig. 6G, H, and I). Large visual fields of each brain section are provided to demonstrate the efficacies of the RB6-8C5 antibody and aminoguanidine treatments in inhibiting the levels of both infiltrating neutrophils and apoptosis as determined by the lack of fluorescent staining.

While the depletion of neutrophils (Fig. 6D, E, and F) had no affect on the level of viral antigen (compare Fig. 6C to A), a marked decrease was observed with respect to the level of apoptosis induced (compare Fig. 6I to G). Sections from aminoguanidine-treated animals also demonstrate that the inhibition of NOS resulted in decreased levels of brain destruction and fewer recruited neutrophils (Fig. 6E) and decreased apoptosis (compare Fig. 6H with G) within the brain parenchyma. These results demonstrate the destructive nature of heightened neutrophil responses within the CNS and suggest that limiting this population, either at their functional or migratory level, affords protection.

T-cell responses differ with A59 versus JHM background genes. Infiltration of the CNS by T cells was analyzed by FACS at days 5 and 7 p.i. for all four viruses (Fig. 7). The numbers of CD4$^+$ and CD8$^+$ T cells are expressed as a percentage of gated cells (Fig. 7A) and as numbers of cells per brain (Fig. 7B). At day 5 p.i., the peak of viral replication, very few infiltrating T cells were found, and all four viruses exhibited similar patterns of CNS infiltration with respect to numbers of CNS lymphocytes, as well as the total number of CD4$^+$ and CD8$^+$ cells. By day 7 p.i., the peak of inflammation in the brain, there were notable differences among the responses to the four viruses.
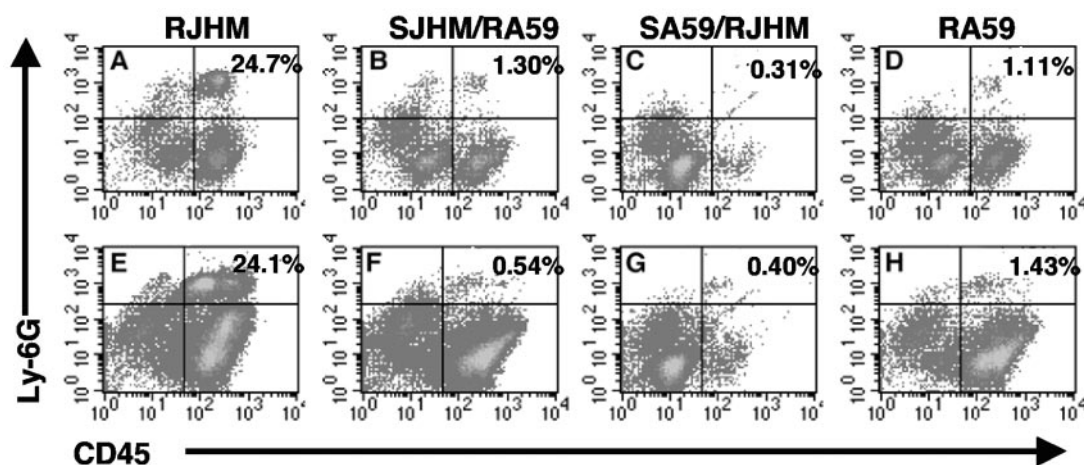

FIG. 5. Infection with RJHM induces a strong neutrophil response in the brain. Lymphocytes pooled from the brains of infected mice sacrificed at days 5 (A to D) and 7 (E to H) p.i. (five per day for each virus) were stained with antibodies against CD45 and Ly-6G and analyzed by FACS. The numbers shown in the upper right-hand corners show the percentages of neutrophils among CNS lymphocytes as measured by staining them with both CD45 and Ly-6G. The images are representative of at least five independent experiments per virus.
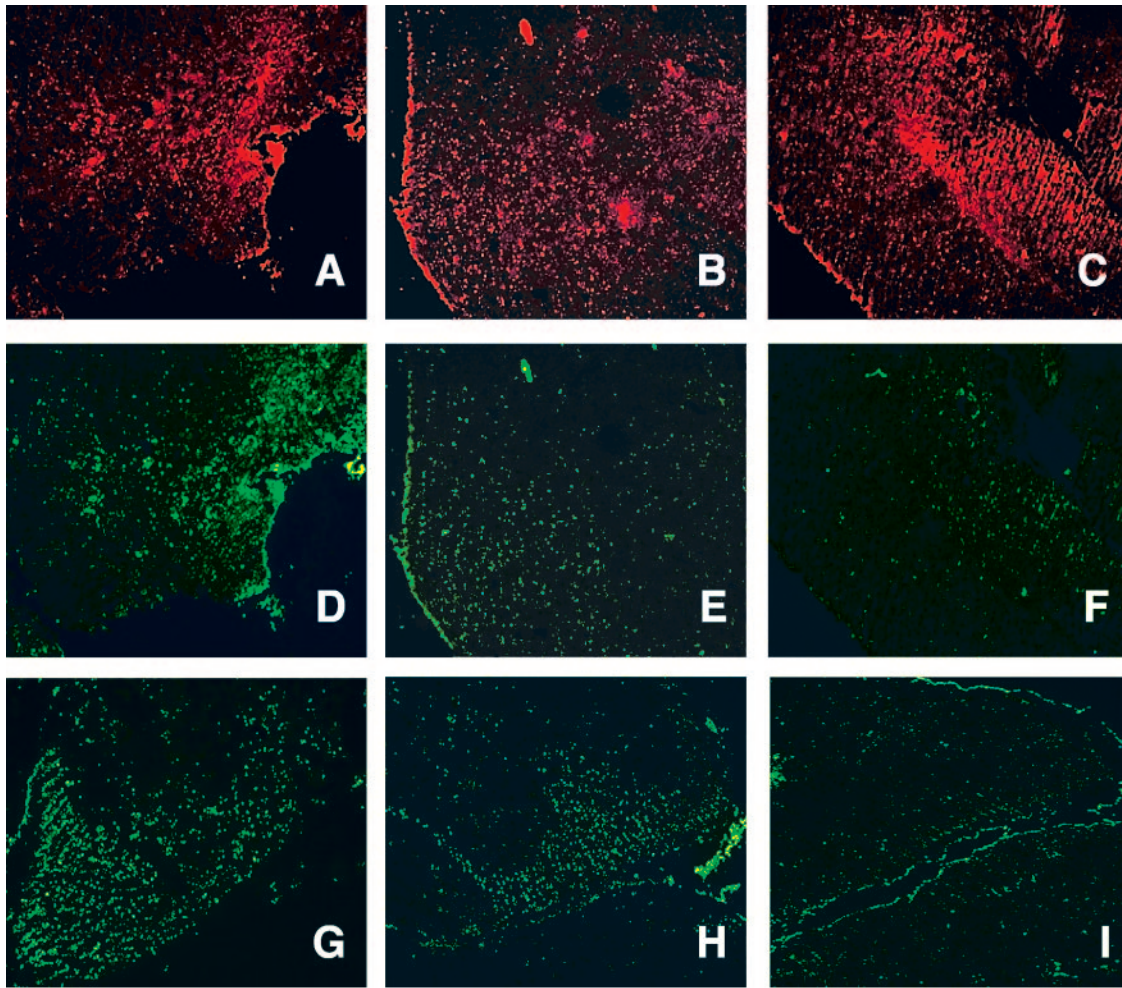
FIG. 6. The depletion of neutrophils or inhibition of their respiratory burst via treatment of mice with aminoguanadine reduces apoptosis levels in the CNSs of RJHM-infected animals. RJHM-infected B6 mice were treated with either PBS (A, D, and G), aminoguanadine (B, E, and H), or the neutrophil-depleting antibody RB6-8C5 (C, F, and I) from day −1 throughout the infectious course until day 5 p.i., at which time the mice were sacrificed, all as described in Materials and Methods. Frozen sagittal brain sections were prepared and evaluated for viral antigen by immunofluorescent staining with polyclonal anti-viral antibody (A, B, and C), for infiltrating neutrophils by staining them with anti-Ly6G (D, E, and F), and for apoptosis by the degree of TUNEL staining, as described in Materials and Methods (G, H, and I). Staining for viral antigen and neutrophils was performed on the same section, while TUNEL staining was performed on an adjacent section. The sections shown are representative of two sections per animal from a total of three animals evaluated for each treatment.

Interestingly, the pattern of T-cell infiltration appeared to segregate with the viral background genes and not the spike, despite the fact that the only two identified MHV H-$2D^b$-restricted T-cell epitopes are in the spike protein (3, 24). Viruses containing the A59 background genes demonstrated markedly heightened levels of CD8$^+$ and CD4$^+$ T-cell infiltration compared to the JHM background-containing viruses (Fig. 7). Both RA59 and SJHM/RA59 demonstrated robust T-cell responses, having similar ratios of CD8$^+$/CD4$^+$ T cells, so that there were about twice as many CD8$^+$ cells as CD4$^+$ T cells. One notable difference between the two viruses was with respect to the total number of lymphocytes infiltrating the brain. As reported previously (27), SJHM/RA59-infected animals had a greater total number of cells than did the RA59-infected animals. In contrast, there was little to no T-cell response within the CNSs of animals infected with the JHM background-containing viruses. With respect to RJHM, the

low number of T cells present at day 7 p.i. was not due to low levels of inflammation in the brain (data not shown). At that time postinfection, when adaptive immunity should have predominated, the heightened numbers of infiltrating neutrophils and macrophages present at day 5 had yet to resolve and were consistently significantly higher in RJHM-infected brains than in those infected with any of the other viruses. The poor T-cell response observed following RJHM infection was likely due to poor antigen presentation and, as such, resulted in impaired viral clearance (K. C. MacNamara and S. R. Weiss, unpublished data). This pattern of high numbers of inflammatory cells despite poor T-cell response observed following RJHM infection was not observed following infection with the other virus expressing JHM background genes, SA59/RJHM, which consistently failed to induce any significant immune response at the 10-PFU dose and had total infiltration numbers consistently 10-fold lower than each of the other viruses. These
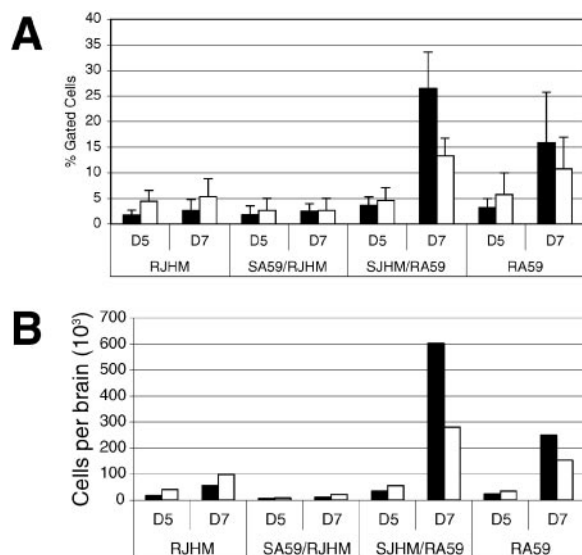
FIG. 7. Evaluation of the T-cell response following MHV infection. Total lymphocytes isolated from the brains of five infected animals per virus were pooled for analysis of surface antigen expression via FACS. The numbers of CD8$^+$ (closed bars) and CD4$^+$ (open bars) cells are presented as (A) percentages (plus standard deviations) of total gated cells following the collection of 10,000 FACS events and (B) the number of cells isolated per brain. The reported values are representative of at least five independent experiments per virus.

results suggest that the high neurovirulence of RJHM is due to the failure to induce a protective T-cell response, dictated by the nonspike background genes, in combination with the ability of JHM spike to mediate extensive and rapid spread in the CNS.

To determine whether the T cells isolated from infected brains were indeed virus specific, they were evaluated for their specificity for the known *H-2D*^{b}-restricted CD8$^+$ T-cell epitopes, S510 (residues 510 to 518) and S598 (residues 598 to 605) (3, 24). While both epitopes are present within the RJHM spike protein, the RA59 spike lacks the immunodominant S510 epitope due to a 52-amino-acid in-frame deletion. To evaluate the epitope-specific responses, cells isolated from the CNS were stimulated ex vivo with virus-specific peptides corresponding to S510 and S598 separately, with epitope specificity measured by intracellular IFN-γ staining as described in Materials and Methods. Figure 8 shows the FACS plots for measurement of IFN-γ^+ and CD8$^+$ T cells (Fig. 8A), as well as the total numbers of CD8$^+$ cells and the number of epitope-specific CD8$^+$ cells per brain in the mice infected with both wild-type and chimeric viruses (Fig. 8B). The two viruses with JHM background genes, regardless of spike, induced very low numbers of total CD8$^+$ T cells in the brain and correspondingly low numbers of epitope-specific cells. In contrast, the A59 background viruses induced appreciable levels of CD8$^+$ T cells, a large number of which were determined to be epitope specific. As expected, for RA59, there was a response following stimulation only with the S598 peptide and not with the S510 peptide, while the cells isolated from the SJHM/RA59-infected animals responded to peptides of both epitopes. While the lack of IFN-γ production contributes to the inability of RJHM-infected animals to clear virus, as well as their high mortality rate, the other spike-expressing virus causes mortality with

slower kinetics than RJHM (Fig. 2), likely due to the induction of a protective virus-specific T-cell response.

DISCUSSION

By comparison of SJHM/RA59 and RA59, we previously demonstrated that the JHM spike protein confers high neurovirulence on a virus with A59 background genes. Furthermore, the increased neurovirulence of SJHM/RA59 over RA59 is associated with increased levels of viral-antigen spread, inflammation, and infiltrating macrophages, as well as greater numbers of infected neurons (27). It is clear, however, that SJHM/RA59 is not as neurovirulent as RJHM. During RJHM infection, the lack of a robust and protective T-cell response and the high levels of macrophages and neutrophils, in combination with the rapid spread, result in a uniformly fatal encephalitis.

Our goals here were to further understand the mechanisms that underlie high neurovirulence and to understand the influence of viral genes, other than spike, on neurovirulence. Thus, we compared the CNS pathogeneses of the four recombinant viruses with both A59 and JHM backgrounds, isogenic other than the spike, as diagrammed in Fig. 1. While all viruses achieved similar titers within the brain during acute infection (data not shown), they differed dramatically with respect to the degree of viral-antigen spread and inflammation induced (Fig. 3). By day 5 p.i., RJHM spread extensively throughout the mid- and hind regions of the brain, inducing very high levels of inflammation and destruction typified by an increased presence of infiltrating immune cells, as well as the spongiotic appearance of the brain. SJHM/RA59 was also found in multiple regions of the mid- and hindbrain, but the viral spread and inflammation appeared more focal (data not shown), with the level of tissue destruction observed in these regions not as extensive. During infection with both RA59 and the SA59/RJHM, very low levels of viral antigen were observed in these regions, with little if any inflammation within the brain parenchyma; these viruses replicate within distinct regions of the brain and are capable of spreading from the midbrain to the olfactory bulb with little perturbation of brain function, as evidenced by a lack of motor skill deterioration within the infected animals. In contrast, by day 5 p.i., the JHM spike-containing viruses infiltrated these same regions and induced neuronal damage that initially presented as severe motor skill deficiencies and ultimately progressed to complete paralysis over the infectious course.

The JHM spike confers the ability to spread rapidly and extensively in the mouse brain (shown here and in reference 27). This is an inherent property of viruses expressing the JHM spike, as such viruses spread more rapidly in primary neuronal-cell cultures, where the immune response is not a factor (27). The JHM spike is capable of mediating receptor-independent fusion and, as a result, theoretically is able to spread to a broader range of cell types within the brain (10). RA59, on the other hand, in cell culture appears to infect and spread only to cells bearing the CEACAM-1 receptor (38, 40, 43). Among the cell types in the brain, CEACAM-1 has been detected only on microglial cells, suggesting a limited tropism for A59 in the brain (19, 29, 41). However, the observation that 50% of infected cells are neurons and astrocytes in the brains of animals
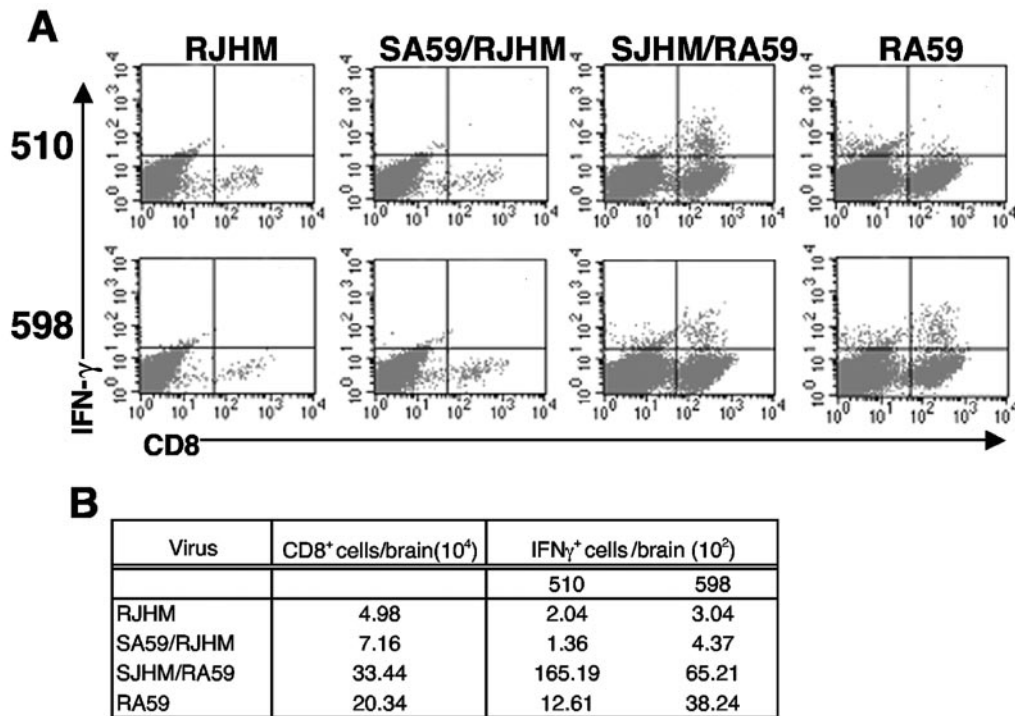
FIG. 8. IFN-γ production by CNS-infiltrating CD8$^+$ cells following infection with wild-type and chimeric viruses. Lymphocytes from the brains of seven mice infected with each virus were pooled and incubated with peptides representing viral S510 and S598 CD8$^+$ T-cell epitopes, as indicated, followed by surface and intracellular staining for CD8 and IFN-γ (see Materials and Methods). (A) Representative panel demonstrating the detection of CD8$^+$, IFN-γ-expressing cells by FACS analysis. (B) Total numbers of CD8$^+$ cells per brain, as well as numbers of S510 and S598 epitope-specific CD8$^+$ cells as measured by an IFN-γ secretion assay. The reported values are the averages of a minimum of three independent experiments per virus.

infected by RA59, as well as SJHM/RA59 (27), indicates that there are likely other receptor-bearing cell types in the brain. There may also be as-yet-unknown pathways for receptor-independent cell-to-cell spread within the CNS, as has been documented for measles virus neuron-to-neuron spread (16).

Both innate and adaptive immunities were evaluated for each recombinant MHV at days 5 and 7 postinfection. While the extent of viral-antigen spread segregates with the spike rather than background genes, the immune response elicited by each MHV strain depends on a combination of both spike and background genes. FACS analyses show that three distinct immune profiles are elicited in a strain-dependent fashion: little innate or adaptive response (SA59/RJHM), little adaptive response (RJHM), or robust adaptive response (RA59, SJHM/RA59); because the evaluations of immune response was performed at times of infection prior to the expected B-cell response, the term adaptive immunity refers only to CD4$^+$ and CD8$^+$ T-cell populations. While SA59/RJHM demonstrated limited spread, caused little destruction, and induced negligible infiltration of the CNS by immune cells at a 10-PFU dose, increasing the viral dose to 50 PFU resulted in levels of viral antigen and CNS-infiltrating T cells (data not shown) that were comparable to the reported values for RA59.

The more rapid viral-antigen spread through the brain following RJHM infection, compared with the other viruses, is accompanied by greater levels of infiltrating neutrophils and macrophages, as well as increased cellular destruction (Fig. 3,

4, and 5). The observation of increased numbers of macrophages within the brains of RJHM-infected animals is consistent with previously reported observations that RJHM-infected animals produced greater levels of macrophage-specific chemokines in the brain, resulting in the infiltration of twice as many macrophages (32, 33). Infiltrating neutrophils were previously reported to have a protective effect for animals infected with an attenuated variant of the JHM strain, v2.1, as evidenced by the observation that antibody depletion of this immune population resulted in shorter time to death (44). However, our data indicate that this may be true only for the attenuated variant strain of JHM and not for the more neurovirulent RJHM used in our experiments (6). Data obtained from the neutrophil depletion studies reported here, using RJHM, suggest that this cell type serves as a destructive force within the inflamed CNS that contributes to the total destruction within the brain parenchyma, as well as to the maintenance of the proinflammatory state. Treatment of RJHM-infected mice with the anti-neutrophil monoclonal antibody RB6-8C5 resulted in complete depletion, to the extent that the neutrophil population was undetectable by FACS, and delayed the time to death by 2 days (data not shown). As further evidence of the destructive nature of neutrophils, the level of apoptosis within the brains of animals treated with either RB6-8C5 or aminoguanadine, an inhibitor of inducible nitrous oxide synthase, was dramatically decreased in comparison to animals receiving only PBS. This leads to the conclusion that the level

of destruction found within the RJHM-infected brain is at least partially immune mediated, with neutrophils serving as mediators of destruction. RJHM's heightened neutrophil recruitment could be due to the complement of cytokines induced following infection. In a study using parental A59 and JHM strains similar to ours, interleukin-1β, a proinflammatory cytokine that mediates the disruption of the blood-brain barrier, was shown to be elevated as early as day 3 p.i. and remained heightened through day 7 p.i. in JHM-infected, but not in A59-infected, brains (32).

In the CNS, clearance of infectious virus requires multiple immunological components, including $CD4^+$ and $CD8^+$ T cells and B cells (12, 18, 34–36, 42). During the acute stage of infection, all four viruses induced an immune response within the CNS; there were, however, striking differences in the T-cell responses and IFN-γ levels among the viruses. The JHM spike protein contains two H-$2D^b$-restricted $CD8^+$ T-cell epitopes, the immunodominant S510 and the subdominant S598 (3), while A59 contains only the subdominant S598 epitope due to a 52-amino-acid deletion within the spike hypervariable region that includes the S510 epitope (24). Both JHM and A59 have similar $CD4^+$ epitopes, three of which are found within the viral spike, and one additional epitope is within the viral membrane protein (24). Based on these findings, it would be expected that both JHM spike-containing viruses would recruit greater numbers of T cells to the CNS, which in turn would lead to higher levels of IFN-γ and result in more efficient viral clearance than would the A59 spike-expressing viruses. This was not the case. Despite the presence of the immunodominant epitope, RJHM recruited fewer $CD8^+$ cells to the CNS than did RA59, with relative numbers being approximately 5- to 10-fold lower than those obtained following SJHM/RA59 and RA59 infections (Fig. 8B). A similar difference in IFN-γ production following infection with A59 and JHM was reported by Rempel et al. (32, 33). Both SJHM/RA59- and RA59-infected animals exhibited virus-specific T cells in the CNS by day 7 p.i.; however, infection with SJHM/RA59 resulted in up to twice as many total T cells than for RA59-infected animals. SJHM/RA59 causes a high degree of mortality despite the mounting of a robust T-cell response and IFN-γ secretion; the high lethality of SJHM/RA59 compared with RA59 is probably due to the rapid spread of the former, mediated by the JHM spike.

While it is possible that the failure of RJHM-infected animals to mount an adaptive response is due to the rapid viral spread associated with this virus, which could lead to killing of antigen-presenting cells early on, we have data (MacNamara and Weiss, unpublished) indicating that a failure in T-cell priming occurs through either the direct infection of dendritic cells (DC) (41) or a failure to activate and thus induce DC migration to the cervical lymph nodes (39). We are currently evaluating the DC populations for their presence and activation states within the brain and cervical lymph nodes.

While our studies clearly support the previous conclusion that the viral spike protein serves as a major determinant of MHV neurovirulence, they also demonstrate that the background genes play a significant role in eliciting an immune response during the acute phase and, hence, in the outcome of the disease. More specifically, we observed that there is a 3-day delay in attaining 50% mortality with SJHM/RA59 compared

with RJHM and that there is some degree of mortality observed in SA59/RJHM-infected animals compared with RA59-infected animals that uniformly survive infection (Fig. 2). Previous data from our laboratory also support the notion that background genes have a major influence on pathogenesis (7, 21). A chimeric recombinant MHV expressing the spike of the highly hepatotropic MHV-2 strain in the A59 background is more virulent than either parental virus; while parental MHV-2 is limited to inducing meningitis within the CNS, this recombinant virus induces encephalitis in a manner similar to A59. However, within the liver, SMHV2/RA59 induces severe hepatitis that is more similar to that induced by the parental MHV-2 than it is to that induced by A59 (7). Similarly, in terms of MHV-induced hepatitis, the JHM background genes are dominant over the A59 spike in that they suppress the ability of SA59/RJHM to replicate in the liver and/or cause disease (21). In both of these examples, it is surprising that the background genes dominate over the spike. It would seem more likely that the spike gene would determine the ability to infect the parenchyma of the brain in the case of the MHV-2/A59 chimera and the liver in the case of SA59/RJHM.

To determine which background genes are responsible for the high neurovirulence of JHM, we selected and characterized A59/JHM chimeric recombinant viruses in which the replicase genes were exchanged. Each of these viruses displayed a pathogenic phenotype nearly identical to that of the parent from which its 3′ end was derived (Navas-Martin and Weiss, unpublished). This suggests that it is the structural genes rather than the replicase that influences tropism and virulence, at least in the context of the A59/JHM chimeric viruses. This is consistent with previous data from our laboratory (15) and the results of Ning and coworkers (22), who showed that the ability to induce the fgl2 host gene, which is a feature of MHV-3-induced fulminant hepatitis, is controlled by the nucleocapsid gene. We are currently evaluating chimeric JHM/A59 viruses in which the JHM nucleocapsid and/or matrix protein will be expressed with or without JHM spike protein in the A59 background. We will use these recombinant viruses to determine which gene(s) is responsible for the high neurovirulence and the poor T-cell immune response characteristic of JHM.

REFERENCES

1. **Andrews, D. M., V. B. Matthews, L. M. Sammels, A. C. Carrello, and P. C. McMinn.** 1999. The severity of Murray Valley encephalitis in mice is linked to neutrophil infiltration and inducible nitric oxide synthase activity in the central nervous system. J. Virol. **73:**8781–8790.
2. **Buchmeier, M. J., H. A. Lewicki, P. J. Talbot, and R. L. Knobler.** 1984. Murine hepatitis virus-4 (strain JHM)-induced neurologic disease is modulated in vivo by monoclonal antibody. Virology **132:**261–270.
3. **Castro, R. F., and S. Perlman.** 1995. $CD8^+$ T-cell epitopes within the surface glycoprotein of a neurotropic coronavirus and correlation with pathogenicity. J. Virol. **69:**8127–8131.
4. **Chua, M. M., K. C. MacNamara, L. San Mateo, H. Shen, and S. R. Weiss.** 2004. Effects of an epitope-specific $CD8^+$-T-cell response on murine coronavirus central nervous system disease: protection from virus replication and antigen spread and selection of epitope escape mutants. J. Virol. **78:**1150–1159.
5. **Compton, S. R., S. W. Barthold, and A. L. Smith.** 1993. The cellular and molecular pathogenesis of coronaviruses. Lab. Anim. Sci. **43:**15–28.
6. **Dalziel, R. G., P. W. Lampert, P. J. Talbot, and M. J. Buchmeier.** 1986. Site-specific alteration of murine hepatitis virus type 4 peplomer glycoprotein E2 results in reduced neurovirulence. J. Virol. **59:**463–471.

7. **Das Sarma, J., L. Fu, J. C. Tsai, S. R. Weiss, and E. Lavi.** 2000. Demyelination determinants map to the spike glycoprotein gene of coronavirus mouse hepatitis virus. J. Virol. **74:**9206–9213.

8. **Deng, X., Y. Wang, J. Chou, and J. L. Cadet.** 2001. Methamphetamine causes widespread apoptosis in the mouse brain: evidence from using an improved TUNEL histochemical method. Brain Res. Mol. Brain Res. **93:**64–69.

9. **Drosten, C., S. Gunther, W. Preiser, S. van der Werf, H. R. Brodt, S. Becker, H. Rabenau, M. Panning, L. Kolesnikova, R. A. Fouchier, A. Berger, A. M. Burguiere, J. Cinatl, M. Eickmann, N. Escriou, K. Grywna, S. Kramme, J. C. Manuguerra, S. Muller, V. Rickerts, M. Sturmer, S. Vieth, H. D. Klenk, A. D. Osterhaus, H. Schmitz, and H. W. Doerr.** 2003. Identification of a novel coronavirus in patients with severe acute respiratory syndrome. N. Engl. J. Med. **348:**1967–1976.

10. **Gallagher, T. M., M. J. Buchmeier, and S. Perlman.** 1993. Dissemination of MHV4 (strain JHM) infection does not require specific coronavirus receptors. Adv. Exp. Med. Biol. **342:**279–284.

11. **Hingley, S. T., J. L. Gombold, E. Lavi, and S. R. Weiss.** 1994. MHV-A59 fusion mutants are attenuated and display altered hepatotropism. Virology **200:**1–10.

12. **Korner, H., A. Schliephake, J. Winter, F. Zimprich, H. Lassmann, J. Sedgwick, S. Siddell, and H. Wege.** 1991. Nucleocapsid or spike protein-specific CD4$^+$ T lymphocytes protect against coronavirus-induced encephalomyelitis in the absence of CD8$^+$ T cells. J. Immunol. **147:**2317–2323.

13. **Ksiazek, T. G., D. Erdman, C. S. Goldsmith, S. R. Zaki, T. Peret, S. Emery, S. Tong, C. Urbani, J. A. Comer, W. Lim, P. E. Rollin, S. F. Dowell, A. E. Ling, C. D. Humphrey, W. J. Shieh, J. Guarner, C. D. Paddock, P. Rota, B. Fields, J. DeRisi, J. Y. Yang, N. Cox, J. M. Hughes, J. W. LeDuc, W. J. Bellini, and L. J. Anderson.** 2003. A novel coronavirus associated with severe acute respiratory syndrome. N. Engl. J. Med. **348:**1953–1966.

14. **Lavi, E., D. H. Gilden, M. K. Highkin, and S. R. Weiss.** 1984. MHV-A59 pathogenesis in mice. Adv. Exp. Med. Biol. **173:**237–245.

15. **Lavi, E., E. M. Murray, S. Makino, S. A. Stohlman, M. M. Lai, and S. R. Weiss.** 1990. Determinants of coronavirus MHV pathogenesis are localized to 3′ portions of the genome as determined by ribonucleic acid-ribonucleic acid recombination. Lab. Investig. **62:**570–578.

16. **Lawrence, D. M., C. E. Patterson, T. L. Gales, J. L. D'Orazio, M. M. Vaughn, and G. F. Rall.** 2000. Measles virus spread between neurons requires cell contact but not CD46 expression, syncytium formation, or extracellular virus production. J. Virol. **74:**1908–1918.

17. **MacNamara, K. C., M. M. Chua, J. J. Phillips, and S. R. Weiss.** 2005. Contributions of the viral genetic background and a single amino acid substitution in an immunodominant CD8$^+$ T-cell epitope to murine coronavirus neurovirulence. J. Virol. **79:**9108–9118.

18. **Matthews, A. E., S. R. Weiss, M. J. Shlomchik, L. G. Hannum, J. L. Gombold, and Y. Paterson.** 2001. Antibody is required for clearance of infectious murine hepatitis virus A59 from the central nervous system, but not the liver. J. Immunol. **167:**5254–5263.

19. **Nakagaki, K., K. Nakagaki, and F. Taguchi.** 2005. Receptor-independent spread of a highly neurotropic murine coronavirus JHMV strain from initially infected microglial cells in mixed neural cultures. J. Virol. **79:**6102–6110.

20. **Navas, S., S. H. Seo, M. M. Chua, J. D. Sarma, E. Lavi, S. T. Hingley, and S. R. Weiss.** 2001. Murine coronavirus spike protein determines the ability of the virus to replicate in the liver and cause hepatitis. J. Virol. **75:**2452–2457.

21. **Navas, S., and S. R. Weiss.** 2003. Murine coronavirus-induced hepatitis: JHM genetic background eliminates A59 spike-determined hepatotropism. J. Virol. **77:**4972–4978.

22. **Ning, Q., L. Berger, X. Luo, W. Yan, F. Gong, J. Dennis, and G. Levy.** 2003. STAT1 and STAT3 alpha/beta splice form activation predicts host responses in mouse hepatitis virus type 3 infection. J. Med. Virol. **69:**306–312.

23. **Ontiveros, E., T. S. Kim, T. M. Gallagher, and S. Perlman.** 2003. Enhanced virulence mediated by the murine coronavirus, mouse hepatitis virus strain JHM, is associated with a glycine at residue 310 of the spike glycoprotein. J. Virol. **77:**10260–10269.

24. **Perlman, S., and L. Pewe.** 1998. Role of CTL mutants in demyelination induced by mouse hepatitis virus, strain JHM. Adv. Exp. Med. Biol. **440:**515–519.

25. **Pewe, L., S. B. Heard, C. Bergmann, M. O. Dailey, and S. Perlman.** 1999. Selection of CTL escape mutants in mice infected with a neurotropic coronavirus: quantitative estimate of TCR diversity in the infected central nervous system. J. Immunol. **163:**6106–6113.

26. **Phillips, J. J., M. M. Chua, E. Lavi, and S. R. Weiss.** 1999. Pathogenesis of chimeric MHV4/MHV-A59 recombinant viruses: the murine coronavirus spike protein is a major determinant of neurovirulence. J. Virol. **73:**7752–7760.

27. **Phillips, J. J., M. M. Chua, G. F. Rall, and S. R. Weiss.** 2002. Murine coronavirus spike glycoprotein mediates degree of viral spread, inflammation, and virus-induced immunopathology in the central nervous system. Virology **301:**109–120.

28. **Phillips, J. J., and S. R. Weiss.** 2001. MHV neuropathogenesis: the study of chimeric S genes and mutations in the hypervariable region. Adv. Exp. Med. Biol. **494:**115–119.

29. **Ramakrishna, C., C. C. Bergmann, K. V. Holmes, and S. A. Stohlman.** 2004. Expression of the mouse hepatitis virus receptor by central nervous system microglia. J. Virol. **78:**7828–7832.

30. **Reed, L. J., and H. Muench.** 1938. A simple method of estimating fifty percent points. Am. J. Hyg. **27:**493–497.

31. **Rempel, J. D., and M. J. Buchmeier.** 2001. Analysis of CNS inflammatory responses to MHV. Role of spike determinants in initiating chemokine and cytokine responses. Adv. Exp. Med. Biol. **494:**77–82.

32. **Rempel, J. D., S. J. Murray, J. Meisner, and M. J. Buchmeier.** 2004. Differential regulation of innate and adaptive immune responses in viral encephalitis. Virology **318:**381–392.

33. **Rempel, J. D., S. J. Murray, J. Meisner, and M. J. Buchmeier.** 2004. Mouse hepatitis virus neurovirulence: evidence of a linkage between S glycoprotein expression and immunopathology. Virology **318:**45–54.

34. **Stohlman, S. A., C. C. Bergmann, R. C. van der Veen, and D. R. Hinton.** 1995. Mouse hepatitis virus-specific cytotoxic T lymphocytes protect from lethal infection without eliminating virus from the central nervous system. J. Virol. **69:**684–694.

35. **Stohlman, S. A., G. K. Matsushima, N. Casteel, and L. P. Weiner.** 1986. In vivo effects of coronavirus-specific T cell clones: DTH inducer cells prevent a lethal infection but do not inhibit virus replication. J. Immunol. **136:**3052–3056.

36. **Sussman, M. A., R. A. Shubin, S. Kyuwa, and S. A. Stohlman.** 1989. T-cell-mediated clearance of mouse hepatitis virus strain JHM from the central nervous system. J. Virol. **63:**3051–3056.

37. **Tepper, R. I., R. L. Coffman, and P. Leder.** 1992. An eosinophil-dependent mechanism for the antitumor effect of interleukin-4. Science **257:**548–551.

38. **Thorp, E. B., and T. M. Gallagher.** 2004. Requirements for CEACAMs and cholesterol during murine coronavirus cell entry. J. Virol. **78:**2682–2692.

39. **Trifilo, M. J., and T. E. Lane.** 2004. The CC chemokine ligand 3 regulates CD11c$^+$CD11b$^+$CD8α^- dendritic cell maturation and activation following viral infection of the central nervous system: implications for a role in T cell activation. Virology **327:**8–15.

40. **Tsai, J. C., B. D. Zelus, K. V. Holmes, and S. R. Weiss.** 2003. The N-terminal domain of the murine coronavirus spike glycoprotein determines the CEACAM1 receptor specificity of the virus strain. J. Virol. **77:**841–850.

41. **Turner, B. C., E. M. Hemmila, N. Beauchemin, and K. V. Holmes.** 2004. Receptor-dependent coronavirus infection of dendritic cells. J. Virol. **78:**5486–5490.

42. **Williamson, J. S., and S. A. Stohlman.** 1990. Effective clearance of mouse hepatitis virus from the central nervous system requires both CD4$^+$ and CD8$^+$ T cells. J. Virol. **64:**4589–4592.

43. **Zelus, B. D., J. H. Schickli, D. M. Blau, S. R. Weiss, and K. V. Holmes.** 2003. Conformational changes in the spike glycoprotein of murine coronavirus are induced at 37°C either by soluble murine CEACAM1 receptors or by pH 8. J. Virol. **77:**830–840.

44. **Zhou, J., S. A. Stohlman, D. R. Hinton, and N. W. Marten.** 2003. Neutrophils promote mononuclear cell infiltration during viral-induced encephalitis. J. Immunol. **170:**3331–3336.